

## Supporting information

### **Co-embedded sulfur vacant MoS<sub>2</sub> monolayer as a promising catalyst for formaldehyde oxidation: a theoretical evaluation**

Thanadol Jitwatanasirikul,<sup>1</sup> Thantip Roongcharoen,<sup>2</sup> Chirawat Chitpakdee,<sup>2</sup> Siriporn Jungsuttiwong,<sup>1,\*</sup> Preeyaporn Poldorn,<sup>1</sup> Kaito Takahashi,<sup>3</sup> Supawadee Namuangruk<sup>2,\*</sup>

<sup>1</sup> *Department of Chemistry, Faculty of Science, Ubon Ratchathani University,  
Warinchamrap, Ubon Ratchathani, 34190, Thailand*

<sup>2</sup> *National Nanotechnology Center, National Science and Technology Development Agency,  
Pathumthani 12120, Thailand*

<sup>3</sup> *Institute of Atomic and Molecular Sciences, Academia Sinica, Taipei 10617*

\*Corresponding Authors: siriporn.j@ubu.ac.th and supawadee@nanotec.or.th

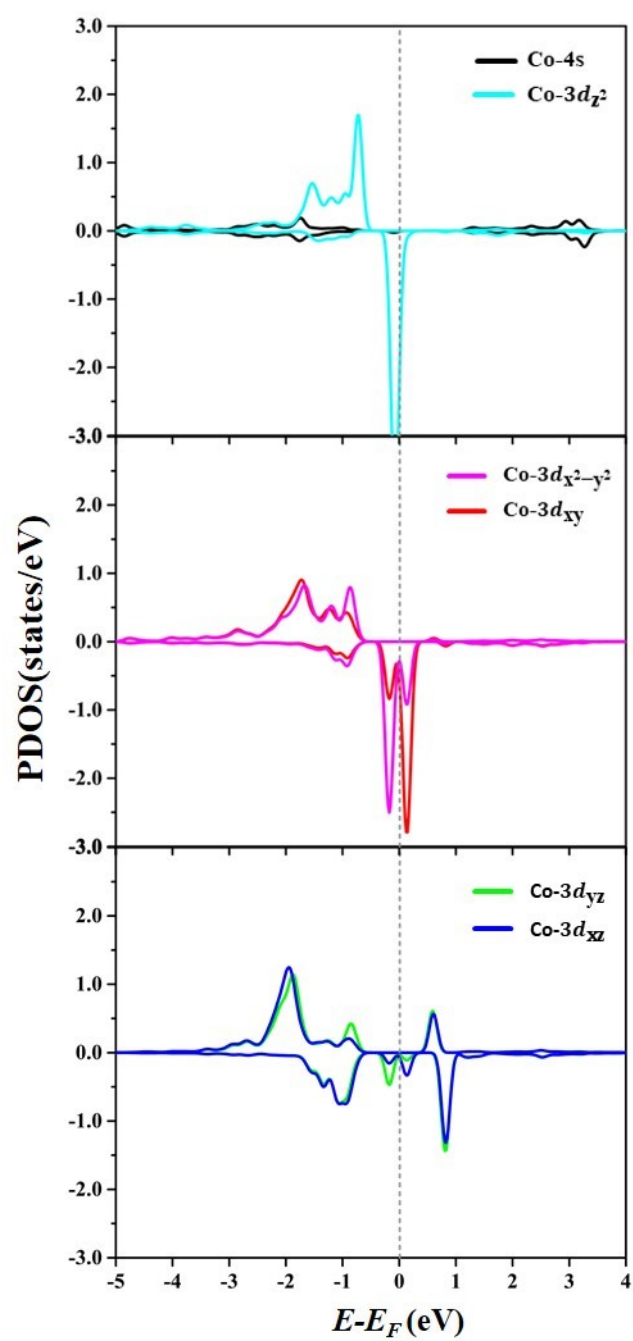


**Figure S1.** Projected density of state for the Co  $4s$ ,  $3d_z^2$ ,  $3d_{x^2-y^2}$ ,  $3d_{xy}$ ,  $3d_{yz}$ ,  $3d_{xz}$  in the  $\text{CoS}_v\text{-MoS}_2$

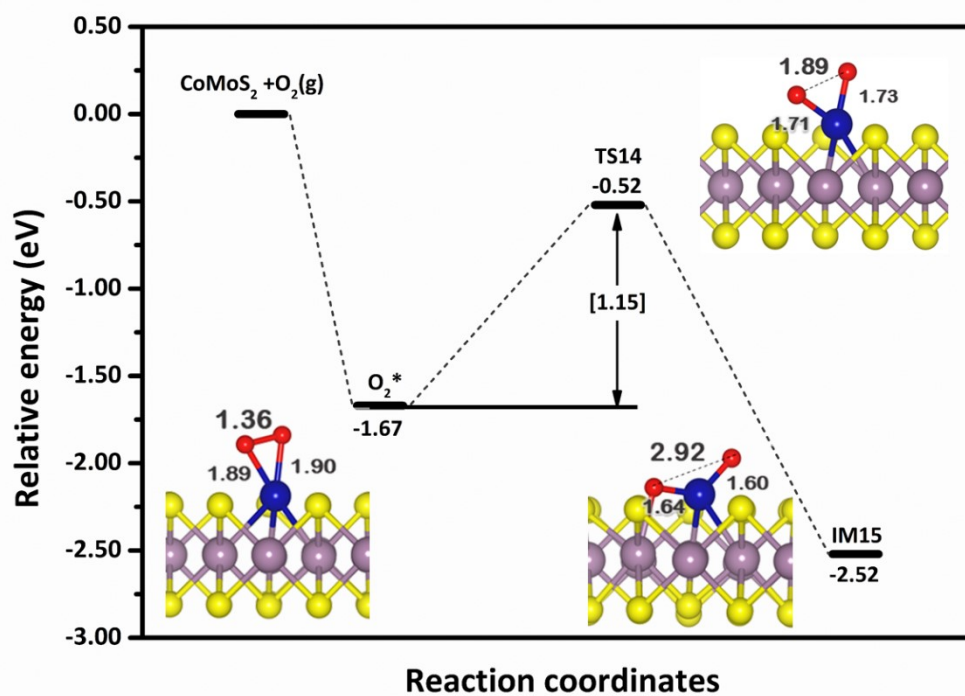


Figure S2. Energy profile and corresponding structures of  $O_2$  dissociation.

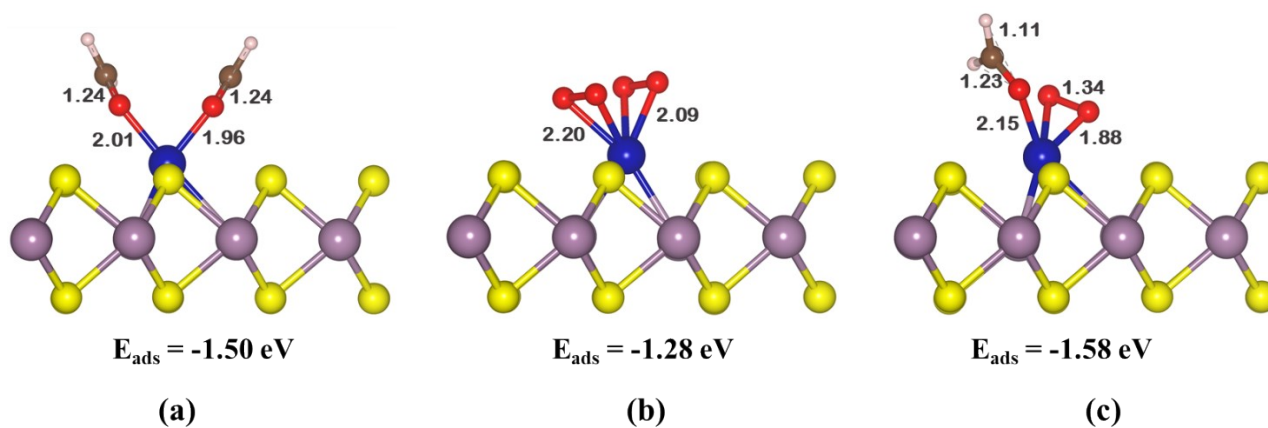


Figure S3. The possible co-adsorption configurations between  $HCHO$  and  $O_2$  on  $Co-MoS_2$

(a) two- $HCHO$  (b) two-  $O_2$  (c) one- $HCHO$  and one-  $O_2$

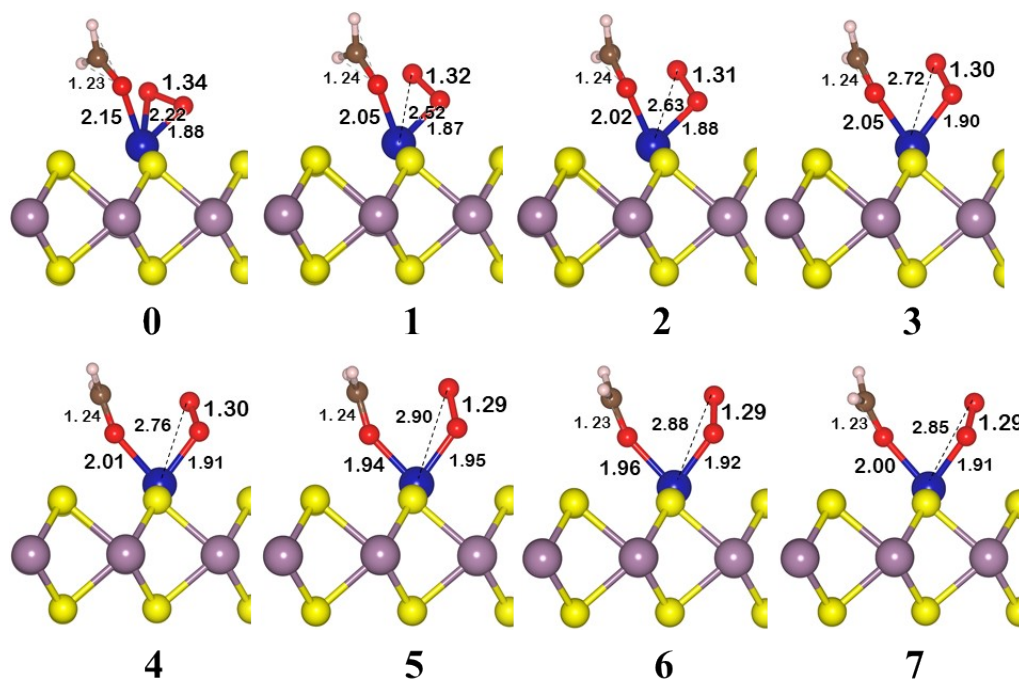
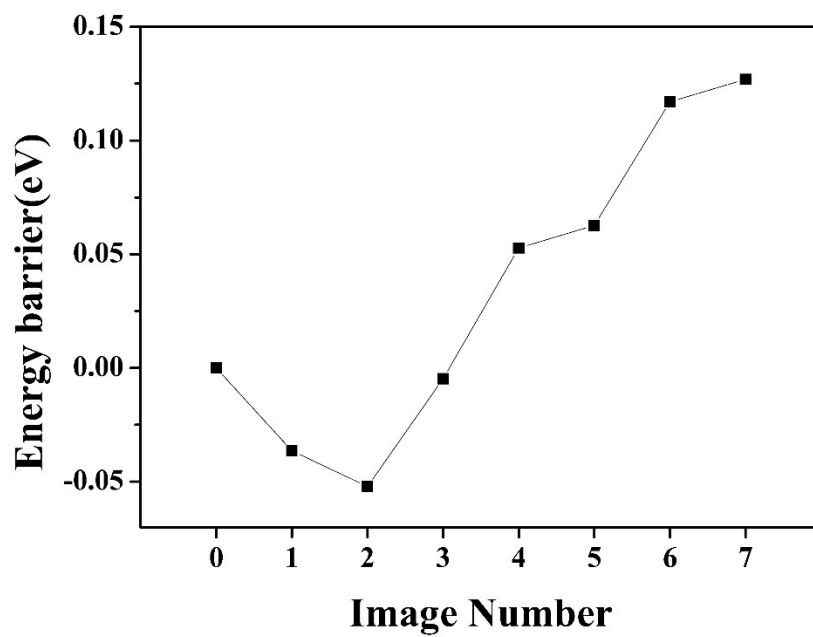
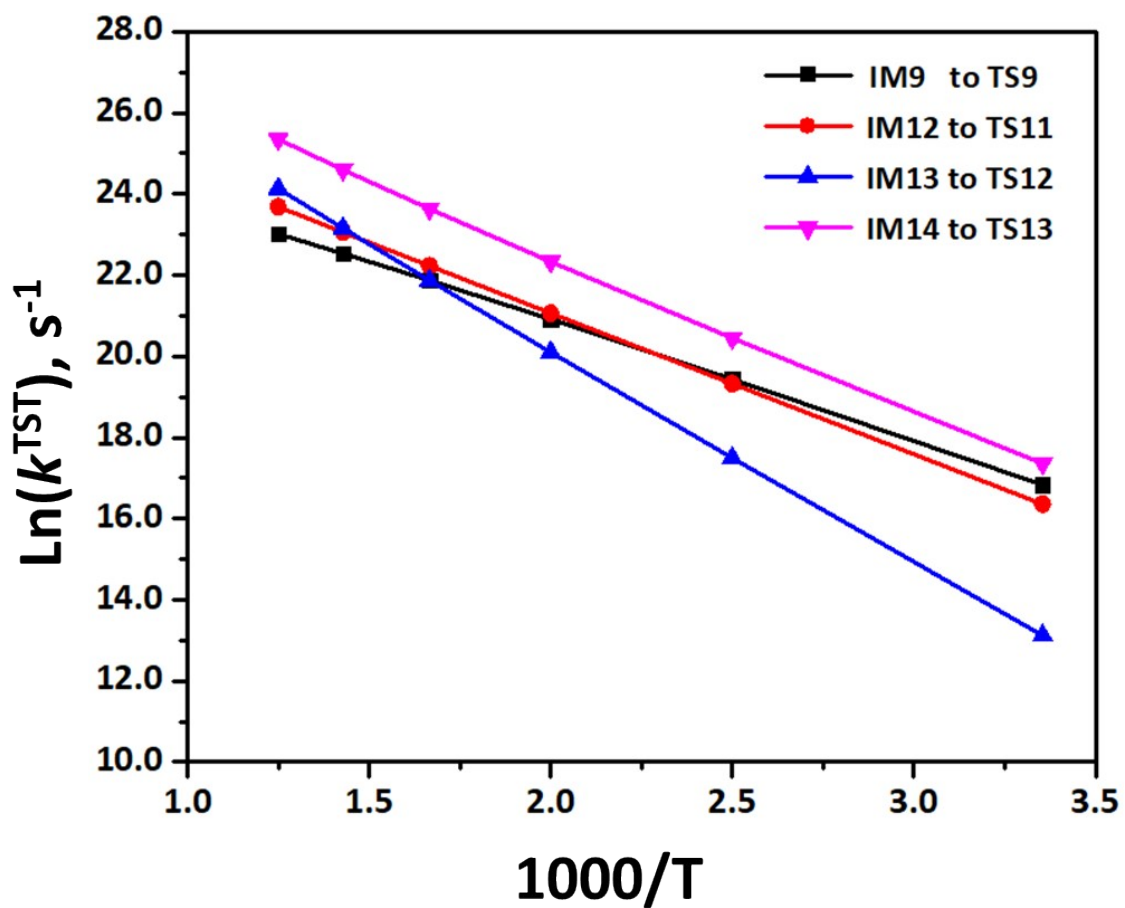


Figure S4. Energy barrier and corresponding structures of IM6 to IM7

**Table S1.** Gibbs free energy barrier ( $\Delta G_b$ , eV) and The reaction rate constants ( $k^{\text{TST}}$ ) for

Species	$E$	$E_b$	$E_{\text{ZPE}}$	$TS$	$C_p dT$	$G$	$G_b$	$k^{\text{TST}}$
IM9→	-391.028		3.511	3.314	1.861	-388.970		
TS9	-390.716	0.312	3.477	3.231	1.823	-388.646	0.32	$2.04 \times 10^7$
IM12→	-393.767		3.490	3.380	1.885	-391.773		
TS11	-393.466	0.301	3.483	3.316	1.864	-391.436	0.34	$1.26 \times 10^7$
IM13→	-393.662		3.448	3.398	1.887	-391.724		
TS12	-393.248	0.414	3.458	3.391	1.877	-391.304	0.42	$4.97 \times 10^5$
IM14→	-393.384		3.443	3.348	1.879	-391.410		
TS13	-393.004	0.380	3.352	3.318	1.871	-391.100	0.31	$3.46 \times 10^7$

elementary steps of the co-adsorption path at 298.15 K.



**Figure S5.** The logarithms of reaction rate constants for rate-determining steps of each elementary step at different temperatures (298.15 – 800 K).

**Table S2.** The reaction rate constants ( $k^{\text{TST}}$ ) and Gibbs free energy barrier ( $\Delta G_b$ ) for rate-determining steps of each path at different temperatures.

Temperature (K)	Consecutive path		Co-adsorption path	
	$k^{\text{TST}}$ (s <sup>-1</sup> )	$\Delta G_b$ eV(kJ.mol <sup>-1</sup> )	$k^{\text{Desorp}}$ (s <sup>-1</sup> )	$\Delta G_b$ eV(kJ.mol <sup>-1</sup> )
298.15	1.12 x 10 <sup>5</sup>	0.46 (44.38)	1.99 x 10 <sup>0</sup>	0.74 (71.30)
400.00	1.03 x 10 <sup>8</sup>	0.39 (37.63)	2.08 x 10 <sup>4</sup>	0.68 (65.86)
500.00	6.34 x 10 <sup>9</sup>	0.32 (30.88)	4.07 x 10 <sup>6</sup>	0.64 (61.32)
600.00	1.06 x 10 <sup>11</sup>	0.25 (24.12)	1.24 x 10 <sup>8</sup>	0.60 (57.45)
700.00	8.28 x 10 <sup>11</sup>	0.17 (16.40)	1.32 x 10 <sup>9</sup>	0.46 (54.17)
800.00	4.00 x 10 <sup>12</sup>	0.10 (9.65)	7.91 x 10 <sup>9</sup>	0.53 (50.89)

System	Magnetic moment of Co in the system ( $\mu_B$ )
$Co_{Sv}-MoS_2$	1.3
R1. HCHO direct decomposition	
HCHO*	0.2
$CH_2^* + O^*$ (IM1)	0.9
$CHO^* + H^*$ (IM2)	0.4
$CO^* + 2H^*$ (FS1)	0.7
$CO^*$ (FS1')	1.2
R2. CO oxidation	
$CO^* + O_2^*$ (IM3)	1.6
$OCOO^*$ (IM4)	1.1
$O^*$	-0.4
$CO_2$ (FS3)	1.3
R3. HCHO oxidation by $O_2$	
$HCHO^* + O_2^*$ (IM6)	1.9
$HCHO^* + O_2^*$ (IM7)	1.8
$CHO^* + OOH^*$ (IM8)	1.2
$OCH_2OO^*$ (IM9)	2.0
$HCOOH^* + O^*$ (IM10)	2.1
$\eta^1-OCHO^* + OH^*$ (IM11)	2.2
$\eta^2-OCHO^* + OH^*$ (IM13)	-2.3
$\eta^1-OCHO^* + OH^*$ (IM4)	2.2
$CO_2^* + H_2O^*$ (FS4)	1.4

**Table S3.** Calculated magnetic moments of Cobalt (Co) in the systems.